OPEN ACCESS

University of BRISTOL

Peer reviewed version

Link to published version (if available):
10.1002/aoc.4111

Link to publication record in Explore Bristol Research
PDF-document

University of Bristol - Explore Bristol Research
General rights

Novel water soluble bis(µ-chloro) bridged Cu(II) binuclear and mononuclear complexes: Synthesis, characterization and biological evaluation

Thangavel Thirunavukkarasu[1] | H. Puschmann[2] | H A. Sparkes[3] | Karuppannan Natarajan[1*] | V. G. Gnanasoundari[4*]

[1]Department of Chemistry, Bharathiar University, Coimbatore 641046, India

[2]Department of Chemistry, Durham University, Durham, DH1 3LE, UK

[3] Department of Chemistry, University of Bristol, Cantock's Close, Bristol, BS8 1TS, UK

[4] Department of chemistry, CBM College, Coimbatore 641042, India

*Corresponding author Email: knatraj66@gmail.com

*Corresponding author Email: vgsoundari@yahoo.com

Abstract

A water soluble chloro bridged binuclear copper(II) complex **(3)** and mononuclear complex **(4)** have been synthesized from chloro substituted 2-oxo-1,2-dihydroquinolin-3-yl-methylene-2 hydroxybenzohydrazide **1** and **2** and $CuCl_2 \cdot 2H_2O$. The structures of the complexes have been determined by single crystal X-ray diffraction. The binding interactions of the ligands and complexes with CT-DNA and protein have been evaluated by absorption and emission spectroscopic method. CT-DNA and ethidium bromide (EB) competitive studies revealed that the compounds could interact with CT-DNA through intercalation binding mode. Interactions of the compounds with BSA were also studied by UV−visible, fluorescence and synchronous fluorescence spectroscopic methods which showed that the compounds had a strong binding affinity with BSA through static quenching process. The cytotoxic effect of the compounds examined on cancer cell lines, such as A549 (lung cancer) and MCF7 (breast cancer) cell lines showed that all four compounds exhibited substantial cytotoxic activity.

Keywords: Schiff base ligands, binuclear copper(II) complex, mononuclear copper(II) complex, DNA, protein binding and cytotoxic activity.

Introduction

In order to assess the potentials of transition metal complexes for applications in bioinorganic chemistry, an extensive amount of work has been carried out recently. In all the biological systems known so far, the metal ions have been found to be coordinated to various types of ligands instead of existing as free ions, and such complexes have shown properties like antibacterial, antifungal, anticancer and antitubercular etc.,[1-10] It is very important to investigate

the interaction of such complexes with bio-molecules such as DNA and protein to determine their ability to function as drugs. In addition, they have to be subjected to *in-vivo* and *in-vitro* biological studies if one wishes to design an active drug. Recently intensive research been focused on using metal complexes as drugs against various diseases. Among the metal complexes, copper complexes have been shown to exhibit significant biological activities.[11-18] Since copper complexes possess biologically accessible redox potentials, high nucleobase affinities and displaying high DNA and protein efficiency, copper complexes are a class of the most frequently studied and documented as metallonucleases.[19-23] Based on this, active searches are on in the synthesis of chloro bridged copper complexes as they show prominent anticancer activity.[24] In the design of such complexes, Schiff base ligands are often used to build multinuclear metal complexes since they show versatile and functionalities [25] besides exhibiting interesting structural, magnetic, biological and catalytic properties.[26] The new complexes have been investigated for their binding with DNA and protein to determine the applications in biotechnology and medicine. Though a few types of interactions of metal complexes with DNA are available, intercalation is one of the most important DNA binding modes, which is related to the antitumor activity of the complex.[27] Moreover, studies on interaction of DNA and protein with metal complexes will provide information of the structural features that determine the therapeutic effectiveness of the complex.[28,29] Given the abundance of copper in nature, it is no surprise that medicinal inorganic chemistry focuses on the copper complexes for their potential applications in cancer biology.[30,31] Though an extensive amount of research has been done in this area, only little amount of work seems to have been done the copper complexes with hydrazone ligands derived from chloro sustituted 2-oxo-1,2-dihydroquinoline-3-carbaldehyde. Hence, we report herein, the synthesis, characterization and biological studies of copper complexes obtained from chloro substituted 2-oxo-1,2-dihydroquinolin-3-yl-methylene-2-hydroxybenzohydrazides with $CuCl_2 \cdot 2H_2O$.

Experimental section

Materials and methods

All the chemicals used are analytical or chemically pure grade and the water used for the experiment was double distilled. 6-chloro-2-oxo-1,2-dihydroquinoline-3-carbaldehyde and 7-chloro-2-oxo-1,2-dihydroquinoline-3-carbaldehyde were prepared according to the literature procedures.[32] Solvents were purified and dried according to the standard procedures. [33] FT-IR

spectra (4000-400 cm^{-1}) for the compounds were recorded on a Jasco FT-IR spectrophotometera and elemental analyses (C, H, N) were performed on Vario EL III Elemental analyzer instrument. Melting points were determined with a Lab India instrument. Electronic absorption spectra were recorded using Jasco V-630 spectrophotometer and emission spectra were obtained using Jasco FP 6600 spectrofluorometer. The ^{1}H NMR spectra were recorded on Bruker AMX 500 at 500 MHz spectrometer. EPR spectra of the complexes were recorded on a Bruker spectrometer operating at the X-band at room temperature. DNA binding, competitive binding fluorescence measurements, protein binding[34,35], cytotoxicity experiments[36] were carried out according to the reported procedures.

Synthesis of the ligands

(7-Chloro-2-oxo-1,2-dihydroquinolin-3-yl-methylene-2-hydroxybenzohydrazide (1): It was prepared by literature method[42] using 2-hydroxybenzohydrazide (1.36 g, 10 mmol) dissolved in warm methanol (20 cm^3) to a methanol solution (30 cm^3) containing 7-chloro-2-oxo-1,2-dihydroquinoline-3-carbaldehyde (1.73 g, 10 mmol). Yield: 89 %. M.p.: 317-319 ºC. Elemental Anal. Calc. for $C_{17}H_{12}ClN_3O_3$ (%): C, 59.75; H, 3.54; N, 12.30. Found (%): C, 59.64; H, 3.43; N, 12.21. FT-IR (cm^{-1}) with KBr disk: 3419 (υ_{OH}), 1595 ($\upsilon_{C=N}$), 1652 ($\upsilon_{C=O}$), 3235 (υ_{NH}): UV-Vis (DMSO), λ_{max} (nm) [ε_{max} (dm^{3}mol^{-1}cm^{-1})]: 388 (309300) (intra-ligand transition). ^{1}H NMR (500 MHz, DMSO-d_6, δ, ppm): δ 12.15 (s, 1H, N(1), H), 12.05 (s, 1H, N(3), H), 11.87 (s, 1H, (-OH)), 8.69 (s, 1H, (HC=N)), 8.51 (s, 1H, (aromatic), H), 7.98–7.86 (m, 2H, (aromatic), H), 7.46 (t, J = 7.0 Hz, 1H, (aromatic), H), 7.37 (s, 1H, (aromatic), H), 7.28 (d, J = 8.1 Hz, 1H, (aromatic), H), 6.96–6.99 (m, 2H, (aromatic), H).

(6-Chloro-2-oxo-1,2-dihydroquinolin-3-yl-methylene-2-hydroxybenzohydrazide (2): 2 was prepared by using 6-chloro-2-oxo-1,2-dihydroquinoline-3-carbaldehyde and 2-hydroxybenzohydrazide. Yield: 89 %. M.p.: 318 ºC. Elemental Anal. Calc. for $C_{17}H_{12}ClN_3O_3$ (%): C, 59.75; H, 3.54; N, 12.30. Found (%): C, 59.60; H, 3.39; N, 12.72. FT-IR (cm^{-1}) with KBr disk: 3417 (υ_{OH}), 1594 ($\upsilon_{C=N}$), 1655 ($\upsilon_{C=O}$), 3234 (υ_{NH}): UV-Vis (DMSO), λ_{max} (nm) [ε_{max} (dm^3 mol^{-1}cm^{-1})]: 267 (47200), 382 (588400) (intra-ligand transition). ^{1}H NMR (400 MHz, DMSO-d_6, δ, ppm): δ 12.20 (s, 1H, N(1), H), 12.08 (s, 1H, N(3), H), 11.85 (s, 1H,(-OH)), 8.70 (s, 1H, (HC=N)), 8.50 (s, 1H, (aromatic), H), 8.04 (s, 1H, (aromatic), H), 7.90 (d, J = 7.8 Hz, 1H, (aromatic), H), 7.59 (d, J = 8.8 Hz, 1H, (aromatic), H), 7.46 (t, J = 7.6 Hz, 1H, (aromatic), H), 7.36 (d, J = 8.8 Hz, 1H, (aromatic), H), 6.94–6.99 (m, 2H, (aromatic), H).

Synthesis of the copper(II) complexes

Complex 3: Ligand **1** (137 mg, 0.5 mmol) in warm N, N-Dimethylformamide (10 cm^3) was added to a methanolic solution (20 cm^3) of CuCl$_2$·2H$_2$O (121 mg, 0.5 mmol). The resulting greenish solution was heated under reflux for 2 hours. Upon cooling, a green colored compound was obtained, which was filtered and washed with methanol and dried. Dark green crystals suitable for single crystal X-ray diffraction studies were obtained by recrystallization from water. Yield: 89 %. M.p.: 342 ºC. Elemental Anal. Calc. for C$_{20}$H$_{18}$Cl$_2$CuN$_4$O$_4$ (%): C, 46.84; H, 3.54; N, 10.92. Found (%): C, 46.64; H, 3.30; N, 12.58. FT-IR (cm^{-1}) with KBr disk: 3417 (υ_{OH}), 1574 ($\upsilon_{C=N}$), 1629 ($\upsilon_{C=O}$). UV-Vis (DMSO), λ_{max} (nm) [ε_{max} (dm^{3}mol^{-1}cm^{-1})]: 270 (516090) (intra-ligand transition); 365 (539410) (ligand to metal charge transfer transition), 394 (531770) (ligand to metal charge transfer transition). EPR (X-band) at room temperature, 'g' value: 2.10.

Complex (4): 4 were prepared by using the same procedure as described for **3** using of **2**. The suitable dark green crystals were obtained for single crystal X-ray diffraction studies upon recrystallization from water/methanol. Yield: 89 %. M.p.: 338 ºC. Elemental Anal. Calc. for C$_{18}$H$_{15}$Cl$_2$CuN$_3$O$_4$ (%): C, 45.82; H, 3.20; N, 8.91. Found (%): C, 45.78; H, 3.16; N, 8.86. FT-IR (cm^{-1}) with KBr disk; 3413 (υ_{OH}), 1578 ($\upsilon_{C=N}$), 1641 ($\upsilon_{C=O}$). UV-vis (DMSO), λ_{max} (nm) [ε_{max} (dm^{3}mol^{-1}cm^{-1})]: 357 (689000) (ligand to metal charge transfer transition), 418 (444100) (metal to ligand charge transfer transition). EPR (X-band) at room temperature, 'g' value: 2.09.

Single crystal X-ray diffraction studies

Single dark green color block-shaped crystals (**3** and **4**) of were recrystallized from water and water/methanol by slow evaporation. A suitable crystal was selected and mounted on a MITIGEN holder in perfluoroether oil on a Xcalibur, Sapphire3 diffractometer. The crystals were kept at T = 120(2) K during data collection. Using Olex2[37], the structure was solved by direct methods in ShelXS and refined in ShelXL[38] using least squares minimization[39]. Crystallographic details are provided in Table 1.

Results and discussion

Synthesis and characterization

Though the reaction of 7-chloro-2-oxo-1,2-dihydroquinolin-3-yl-methylene-2 hydroxybenzohydrazide with CuCl$_2$·2H$_2$O yielded a chloro bridged binuclear copper complex, a very similar reaction with 6-chloro-2-oxo-1,2-dihydroquinolin-3-yl-methylene-2 hydroxybenzohydrazide resulted in a mononuclear complex. It is quite surprising and difficult to

explain how the change in the position of chloride in the ligand can lead to the formation of two types of complexes under a similar reaction condition shown in **Scheme 1**. They have been characterized by IR, elemental analysis, UV−visible, fluorescence spectroscopy, EPR and ^{1}H NMR. The molecular structures of the complexes have been determined by single crystal X-ray studies, which showed that they are square pyramidal geometry. The compounds are air stable in the solid phase and highly soluble in water and also soluble in methanol, ethanol, dimethylformamide and dimethylsulfoxide.

Spectroscopy

The electronic spectrum of ligands showed two resolved bands one at 267 and the other at 382-388 nm, which are assigned to intra ligand charge transfer transitions. Complex **3** showed three peaks in the region between 270 and 365-394 nm. The band at 270 nm is assigned to intra ligand transition, while the band in the region 365-394 is assigned to the ligand-to-metal charge transfer transition. Complex **4** showed two absorption bands at 357-418 nm assigned to ligand-to-metal charge transfer transition and metal-to-ligand charge transfer transition.[40] The FT-IR spectra of the **1** and **2** displayed characteristic absorption bands in the regions 3419–3417, 3235–3234, 1652–1655 and 1595–1594 cm^{-1} due to (-OH), (-NH), (C=O) and (C=N) vibrations respectively. The bands due to (-NH) vibrations observed for the free ligands disappeared completely, which indicating enolisation with (-NH and C=O) followed by deprotonation leading to coordination through O atom. The phenolic -OH stretching frequency did not show any significant change in the spectra of complexes compared to the ligands. The azomethine(C=N) stretching frequency have been shifted to lower frequency of 1574-1578 cm^{-1} in the complexes, which indicated that the N atom of C=N coordinated to the metal ion. The IR result suggested that the quinoline based hydrazone ligands behave as monobasic tridentate (ONO) chelating ligands in the complex **3** and **4**.[41] In the ^{1}H NMR spectra of the ligands showed in Figures S1 & S2. The signal due to –NH proton was observed as a singlet at δ 12.15 and 12.20 ppm in the spectra of **1** and **2**. The two singlets appeared at δ 11.87 and 11.85 ppm for phenolic -OH. A sharp singlet's appeared at δ 8.69 and 8.70 ppm, which corresponds to azomethine protons of the ligands **1** and **2** respectively. The resonance due to aromatic protons of the ligands at δ 12.05 and 6.97 ppm.[42,43] Copper complexes are EPR active due to the presence of an unpaired electron. The +2 oxidation state of the copper ion in the complexes was confirmed by X-band EPR the measurements at room temperature. The copper complexes **3** and **4** showed well resolved isotropic resonance typical of

square pyramidal Cu(II) system showed in Figures S3 & S4. The trend in the g values 2.10 and 2.09 for complex **3** and complex **4** respectively. From these values, we suggest that the unpaired electron of Cu(II) ion is present in the $d_{x^2-y^2}$ orbital.
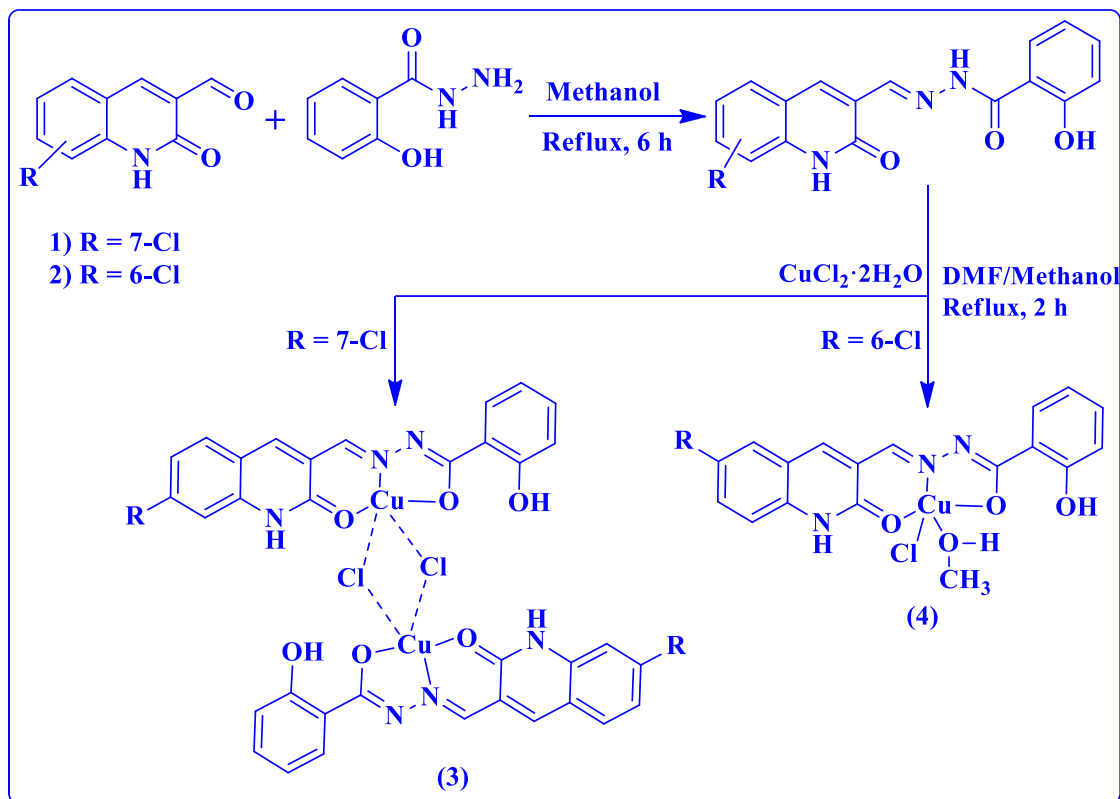
Scheme 1. Synthesis of ligands and their copper(II) complexes.

Crystallography

Crystal data and structure refinement for **3** and **4** are shown in Table 1. The complex **3** crystallized with a distorted square pyramidal monoclinic Cu(II) metal centre with $P2_1/c$ space group. Two units of the ligands coordinated to the metal through two oxygen and one nitrogen atoms leading to a dimeric complex with two chloride ligands bridging the two copper ions. The complex, which stacks through the chlorine atom of the metal ion, resulted in centrosymmetric dimer. Each monomeric unit interacts with another copper centre by a symmetric double chloro bridge forming a Cu_2Cl_2 rectangular core. The double chloro bridged(μ-Cl) connecting both Cu(II) ions is symmetric because each Cu(II) center is closer to its own chlorine atom [Cu_1–Cl_2 = 2.2394(7) Å. The dihedral angle between the mean planes of the five-member chelate ring and

the six-member are O1-Cu1-O2 is 164.03(8) (º). The molecular structure of the complex 3 showed in Figure 1. Intramolecular hydrogen bonding exists between the hydroxyl OH and the diazine N that is not coordinated to the Cu. In addition, intermolecular hydrogen bonding is present between N, N-dimethyl formamide and an amide N showed in Table 2 and Figure 2. π-π stacking interactions are also present with just the C4-C9 rings creating stacks in the *c*-axis direction, the rest of the molecule are distorted away from each other and not overlapping showed in Table 3 and Figure 3. Important bond lengths and bond angles are tabulated in Table S1.

Complex **4** crystallized with a distorted square pyramidal monoclinic Cu(II) metal centre with *P2₁*=c space group. The complex contains the ligand coordinated as monobasic ONO tridentate manner with the chloride and methanol occupying the fourth and fifth coordination sites. There are two independent molecules in the asymmetric unit. In one of them, a molecule of methanol is coordinated in the Jahn-teller site while there is disorder between a methanol and water in the other molecule. The angle between the mean planes of the four-member chelate ring and the six-member are O1-Cu1-O2 is 169.42(14) and O7-Cu1-O6 is 170.21(14) (º). The molecular structure of the complex **4** showed in Figure 4. Important bond lengths and angles for both the complexes are summarized in the Table S1.
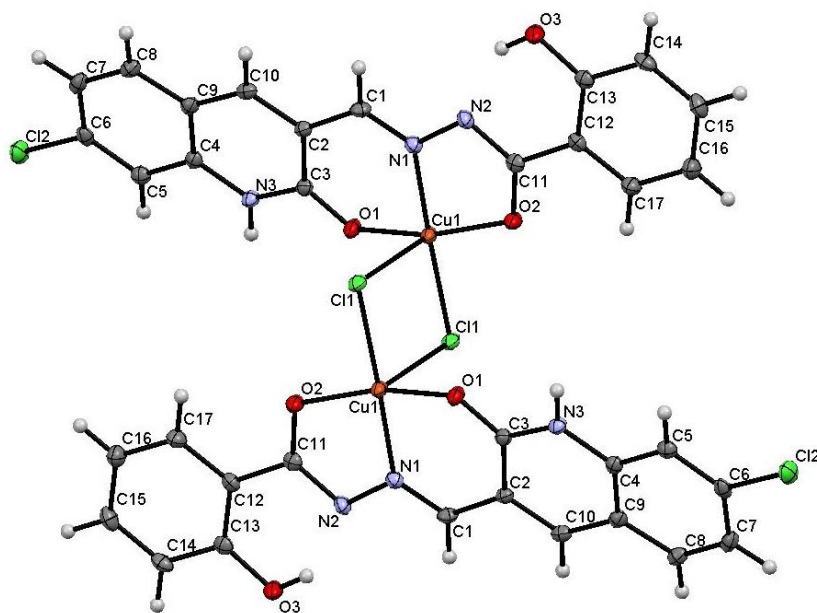

Figure 1. Molecular structure of complex (**3**). Thermal ellipsoid plot for **3** with ellipsoids depicted at the 50% probability level. N, N-Dimethylformamide solvent molecule in the lattice is omitted for clarity.
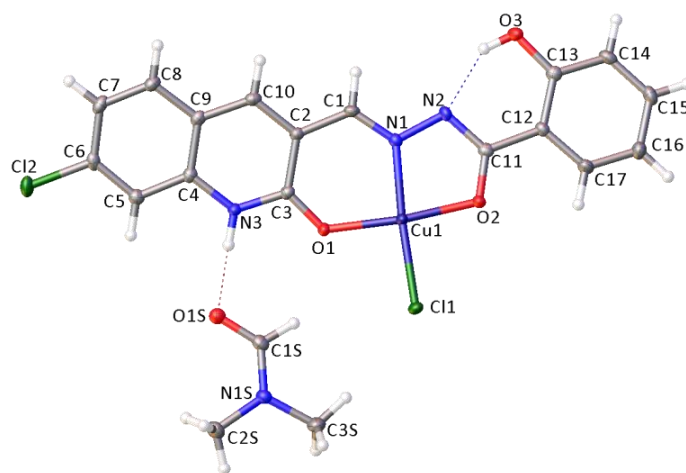
Figure 2. Intramolecular and intermolecular hydrogen bonding interactions of complex **3**.
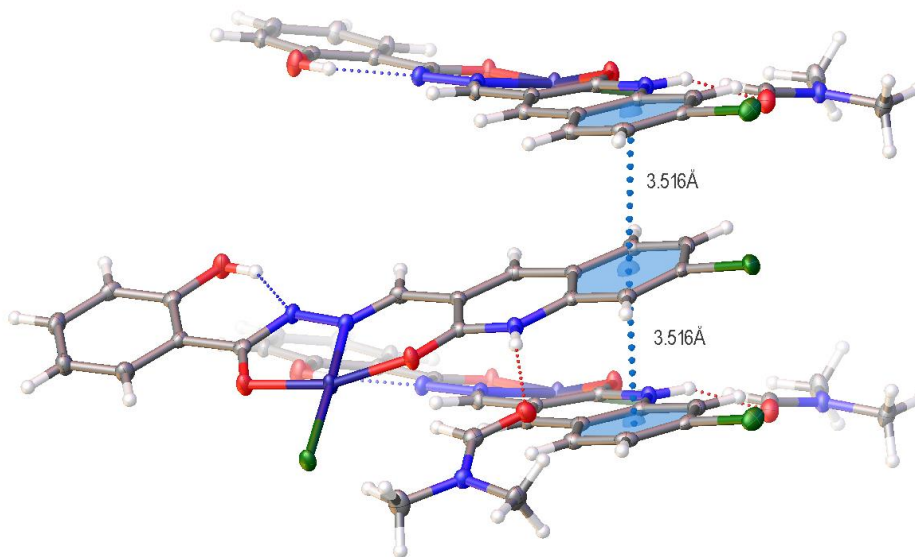

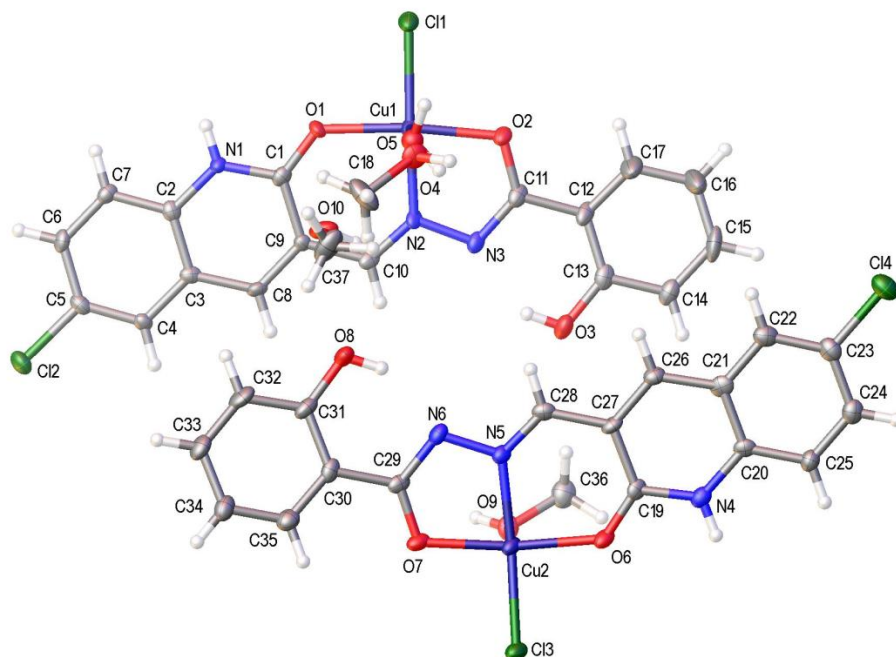**Figure 3**. The π-π interactions of complex **3**.

Figure 4. Molecular structure of complex (**4**).

Table 1: Crystal data and structure refinement for complex **3** and **4**

Compound	3	4
Empirical formula	$C_{20}H_{18}Cl_2CuN_4O_4$	$C_{18}H_{15}Cl_2CuN_3O_4$
Formula weight	512.82	474.47
Temperature/K	120(2)	120(2)
Crystal system	monoclinic	monoclinic
Space group	$P2_1/c$	$P2_1/c$
a/Å	15.5275(5)	16.1733(7)
b/Å	18.4180(6)	10.8489(5)
c/Å	7.0255(3)	21.7111(11)
α/°	90	90
β/°	93.946(4)	100.398(5)
γ/°	90	90
Volume/Å^3	2004.43(13)	3746.9(3)
Z	4	8
ρ_{calc}g/cm^3	1.699	1.682
μ/mm^{-1}	1.394	1.483
F(000)	1044.0	1924
Crystal size	$0.20 \times 0.09 \times 0.06$	$0.33 \times 0.09 \times 0.08$
2θ range for data collection/°	3.436 to 54.998	3.436 to 54.998
Reflections collected	18765	30288

R_{int}	0.0483	0.0877
Data/restraints/parameters	4593/0/283	7359/0/530
Goodness-of-fit on F^2	1.108	1.061
Final R indexes [I>=2σ (I)]	$R_1 = 0.0411$, $wR_2 = 0.0848$	$R_1 = 0.0634$, $wR_2 = 0.1622$
Final R indexes [all data]	$R_1 = 0.0533$, $wR_2 = 0.0949$	$R_1 = 0.1051$, $wR_2 = 0.1622$
Largest diff. peak/hole / e $Å^{-3}$	0.47/-0.35	2.04/-0.73

Table 2. Hydrogen Bond information.

D	H	A	d(D-H)/Å	d(H-A)/Å	d(D-A)/Å	D-H-A/deg
O3	H3	N2	0.84	1.87	2.603(3)	145.9
N3	H3A	O1S	0.88	1.88	2.703(3)	155.4

Table 3. π-π stacking interactions

Ring	Ring	Centroid-centroid distance (Å)	Shift distance (Å)
C4-C9	C4-C9^i	3.516	1.011
C4-C9	C4-C9^{ii}	3.516	0.926

i +x, ½-y. -1/2+z, ii +x, ½-y, ½+z

DNA binding studies

Electronic absorption titration: Since DNA is an important cellular target for many metallo-drugs in treating of multiple pathologies including cancer, an investigation into the binding of ligands and metal complexes with DNA is an important one.[44,45] This can be easily done by observing the changes in the electronic absorption spectra of the compounds as a function added DNA concentration and hence we carried out the interaction of our compounds (10 µM) with DNA (0-100 µM) and the results obtained are shown in Figure 5. It has been seen that there was a significant change in the absorption summary of **1–4** on sequential addition of DNA. From the spectra shown in Figure 5, one can notice that the intensity of absorption decreases resulting in hypochromism with a small blue shift. This change indicates that there exists an intercalative mode of binding due to the strong stacking interaction between an aromatic chromophore and the base pairs of DNA.[46] The extent of shift and hypochromism are normally found to correlate with the intercalative binding strength. The magnitude of hypochromism is in the order of **3** > **4** > **1** > **2**, which reflects the DNA binding affinities of the compounds. Further, the intrinsic binding constant of the compounds with CT-DNA can be determined using the equation[47] [DNA]/[ε_a-ε_f] = [DNA] / [ε_a-ε_f] + 1/K_b[ε_a-ε_f], where [DNA] is the concentration of DNA in base

pairs. Each set of data, when fitted into the above equation, gave a straight line with a slope of $1/(\varepsilon_a-\varepsilon_f)$ and an y-intercept of $1/K_b$ $(\varepsilon_a-\varepsilon_f)$ Figure 6. The magnitudes of intrinsic binding constants K_b calculated values are $0.2753 \times 10^6 \pm 0.3$, $0.2575 \times 10^6 \pm 0.27$, $1.0835 \times 10^6 \pm 0.32$ and $0.5019 \times 10^6 \pm 0.29$ M^{-1} for the ligands and complexes. Complex **3** showed better DNA binding affinity compared to the other compounds. It is also noted that the addition of CT-DNA to the complex **3** led to an isobestic point appearing at 291 nm. The appearance of the isosbestic points suggests that a chemical equilibrium exists between the DNA and compound. The enhanced binding of **3** may be due the presence of the extension of the π system of the intercalated ligand which leads to a greater planar area of the dimeric complex **3** than the free ligands and the complex **4**.
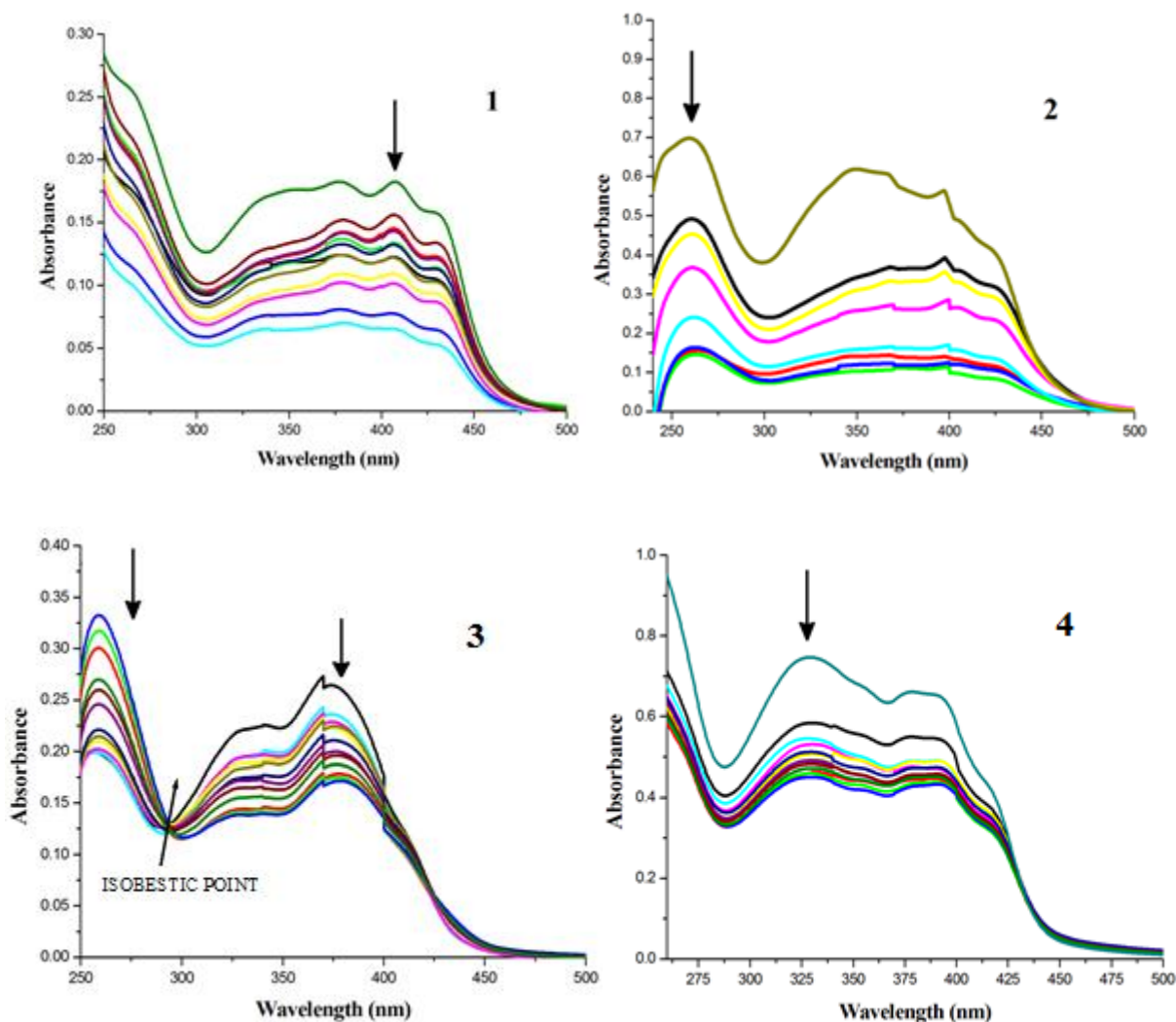

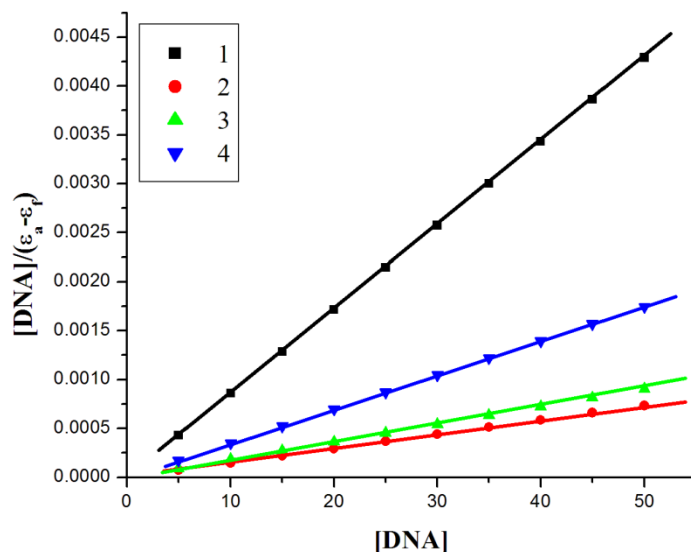**Figure 5**. Absorption titration of the compounds with CT-DNA.

Figure 6. Plot of [DNA] / [ε_a-ε_f] *versus* [DNA].

EB displacement study

The nature of exact binding of the compounds with DNA cannot be obtained from electronic spectral data since the compounds showed no fluorescence at room temperature in solution or in the presence of CT-DNA. To obtain concrete information, one need to measure emission spectra and therefore, the extent of quenching of fluorescence of EB bound to CT-DNA has to be used to determine the binding of the second molecule to DNA.[48] This competitive method usually gives indirect evidence for the mode of DNA binding.[49] Hence, we carried the recording of the emission spectra by adding an increasing amount of our compounds to EB bound DNA excited at 624 nm. The emission spectra of EB-DNA in the absence and presence of the compounds **1–4** are shown in Figure 7. A competitive binding of the ligands and copper complexes to CT-DNA resulted in the displacement of bound EB, and as a consequence, the emission intensity decreased due to intercalative binding to CT-DNA. The relative order of binding was obtained from the linear Stern–Volmer equation[50], $I_0/I = 1 + K_q[Q]$. Here, I_0 and I are the fluorescence intensities in the absence and presence of the compounds, K_q is a linear Stern–Volmer quenching constant, and [Q] is the total concentration of a compounds to that of DNA. The value of K_q is given by the ratio of the slope to the intercept in a plot of I_0/I versus [Q] showed in Figure 8. The EB-DNA fluorescence quenching property constant values obtained are $1.12 \times 10^3 \pm 0.002$, 1.13

$\times$ 10^3 $\pm$ 0.002, 3.04 $\times$ 10^3 $\pm$ 0.011 and 2.88 $\times$ 10^3$\pm$ 0.01 M^{-1}, which indicate the extent of displacement of ethidium bromide by the compounds.
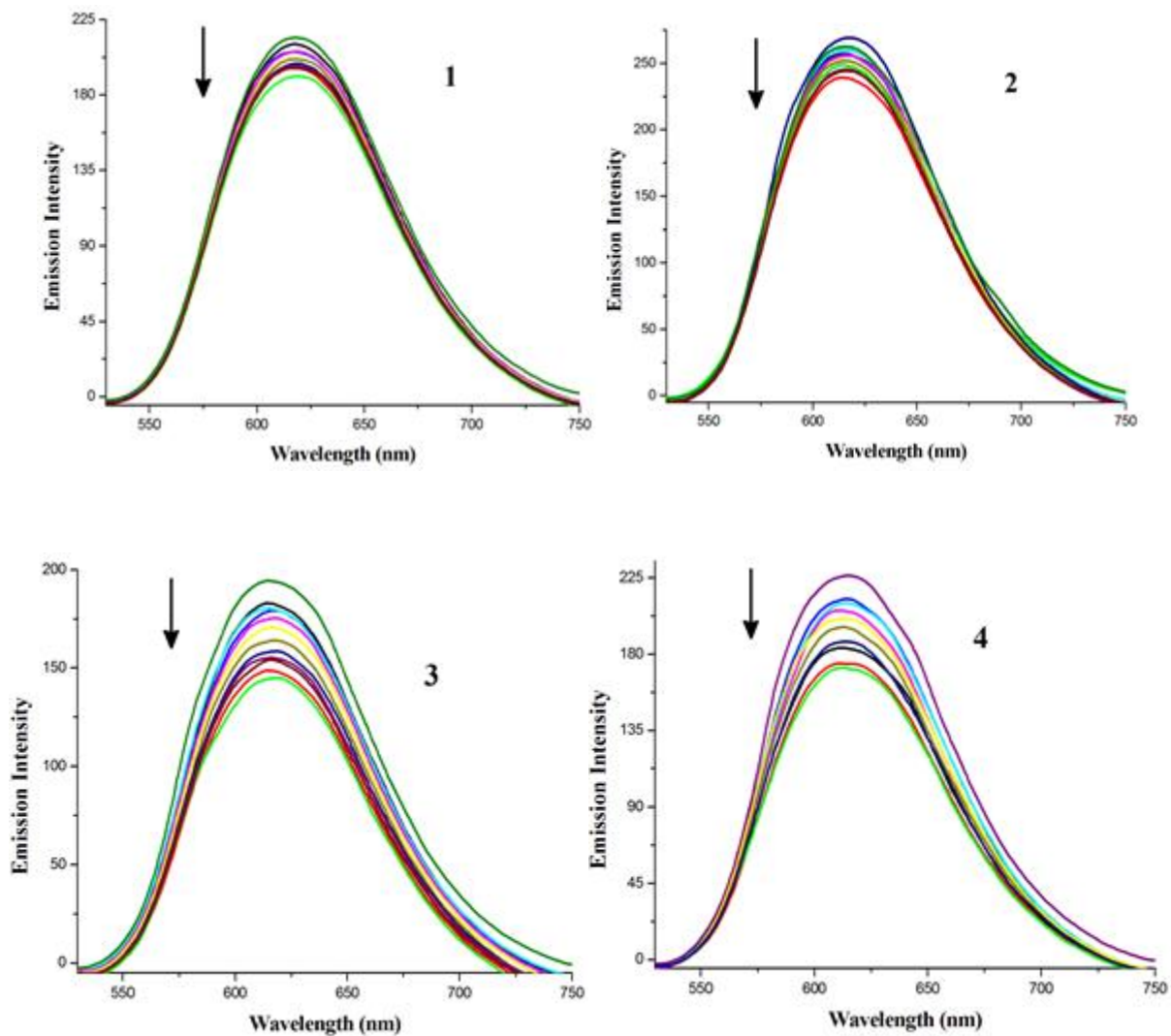

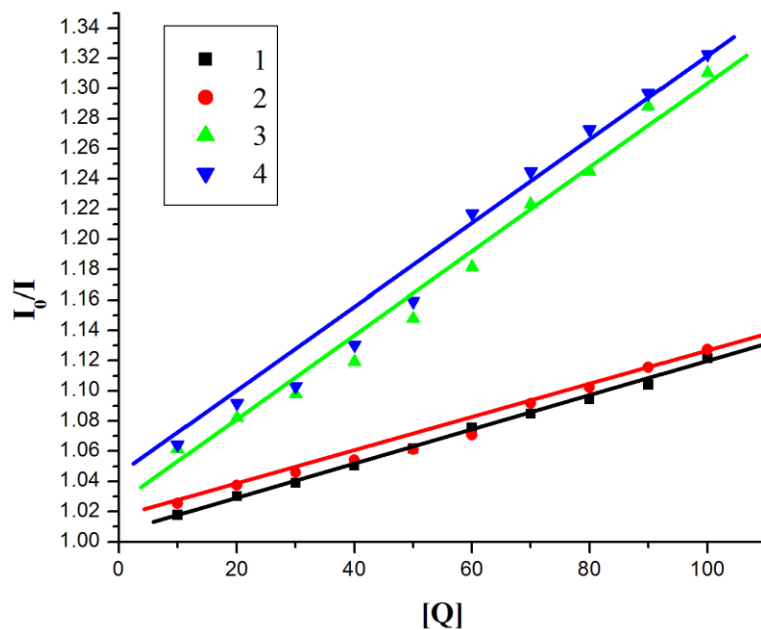**Figure 7.** Fluorescence titration of the compounds with EB-DNA.

Figure 8. Stern–Volmer plot of the compounds with CT-DNA.

Protein binding studies

Fluorescence and absorbance studies: In addition to the studies carried out so far, protein binding study is also essential in determining the ability of a compound to be an active drug. Information on this can be obtained by interacting the ligands and the corresponding copper complexes with serum albumin through fluorescence spectroscopic studies by measuring the intrinsic fluorescence of BSA. Figure 9 shows the changes observed in the intensity fluorescence emission of BSA on the addition of increasing amount of the test compounds. The fluorescence properties of BSA arise from its intrinsic characteristics, mainly due to the presence of tryptophan and tyrosine residues.[51] Addition of the test compounds to the solution of BSA resulted in considerable decrease in the fluorescence intensity of BSA at 348 nm accompanied by a 1,2,1 and 2 nm blue shift for the compounds **1-4**. The fluorescence quenching data were analyzed with the Stern−Volmer equation and Scatchard equation showed in Figure 10, 11 and Table 4. The quenching constant K_{SV} value was obtained from the plot of I_0/I *versus* [Q] in Stern−Volmer equation. Due to the fact that the active site in the protein is buried in a hydrophobic environment a blue shift has been observed. This result suggested a definite interaction of all the four compounds with the BSA protein and the value of '*n*' indicates the

existence of a single binding site in BSA for the test compounds. The larger values of K_q for the complex **3** indicates that it interacts strongly with BSA protein.[52,53]
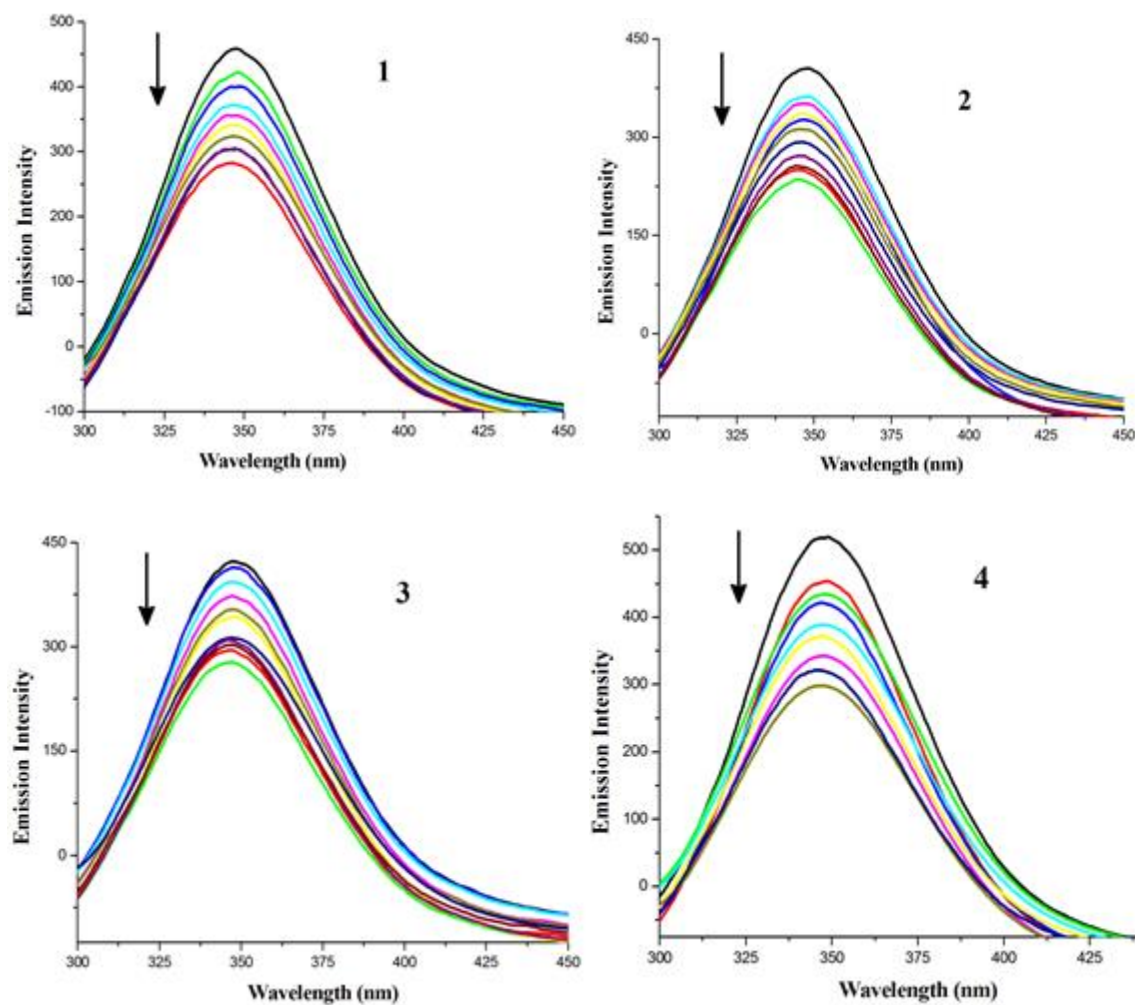

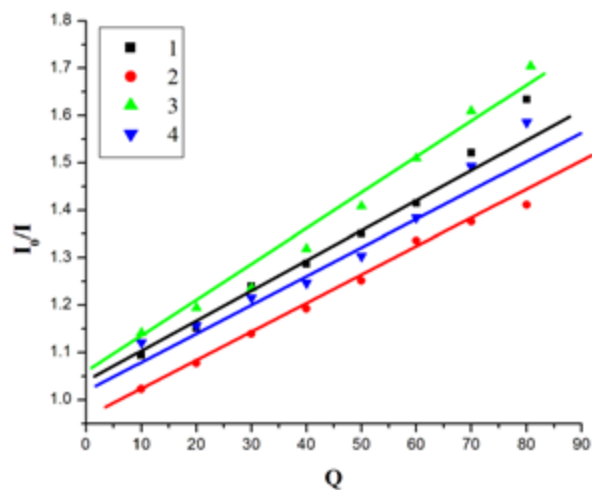**Figure 9**. The fluorescence titration of BSA with the compounds.

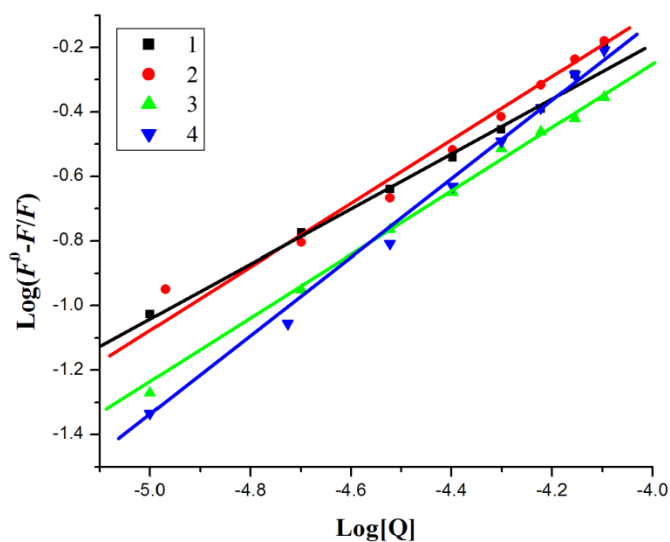**Figure 10.** Stern–Volmer plot of the compounds with BSA.

Figure 11. Scatchard plot of the compounds with BSA.

Table 4. Binding constant (K_{bin}), quenching constant (K_{SV}), and number of binding sites (n) for the interactions of compounds with BSA.

Compound	K_{bin} (M^{-1})	K_{KSV} (M^{-1})	n
1	$6.28 \pm 0.14 \times 10^2$	$7.4 \pm 0.02 \times 10^3$	0.69
2	$3.30 \pm 0.10 \times 10^2$	$5.65 \pm 0.02 \times 10^3$	0.81
3	$1.43 \pm 0.17 \times 10^3$	$8.49 \pm 0.02 \times 10^3$	1.01
4	$9.69 \pm 0.15 \times 10^2$	$6.89 \pm 0.02 \times 10^3$	0.99

The mechanism of quenching is usually classified as dynamic and static. Static quenching refers to fluorophore-quencher complex formation in the ground state, and the dynamic quenching refers to a process in which the fluorophore and quencher come into contact during the transient existence of the excited state. The easiest method to determine the type of quenching is UV-Vis absorption spectroscopy. The UV-Vis spectra of BSA in the absence and presence of the complexes are shown in Figure 12. The addition of the compounds to a fixed concentration of BSA led to a gradual decrease in the intensity of BSA absorption at the same wavelength due to the interaction between the complexes and protein, which is mainly ascribed to the static quenching.[54]
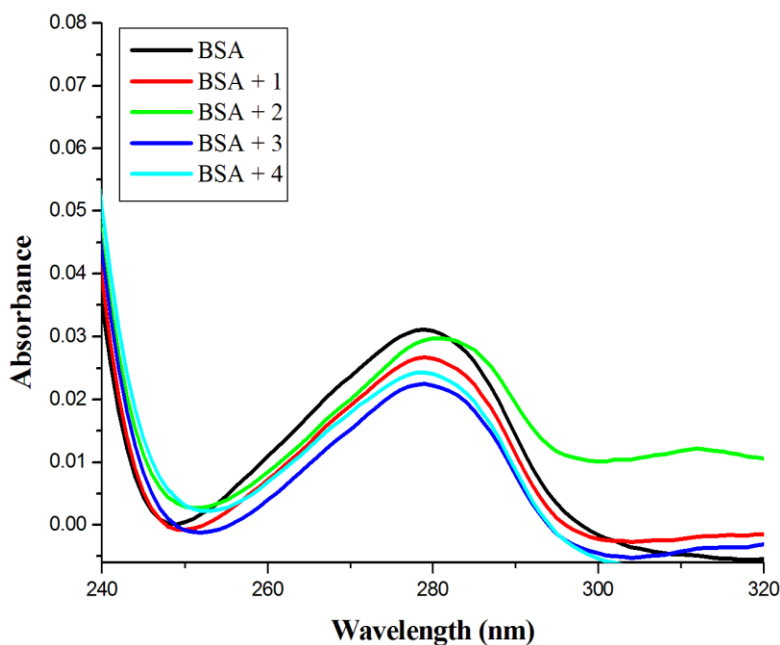

Figure 12. Absorbance titration of the compounds with BSA

Synchronous fluorescence spectra

It further necessary to look at the structural changes occurring to bovine serum albumin upon the addition of ligands and complexes and to find out that synchronous fluorescence spectral studies of bovine serum albumin has to be carried out. It is a known fact that the fluorescence of bovine serum albumin is normally due to the presence of tyrosine, tryptophan and phenylalanine residues and synchronous fluorescence spectral studies of serum albumin will indicate the presence of any above said three residues. The type of chromophore indicate in the interaction

can be inferred from the difference between the excitation wavelength and emission wavelength ($\Delta\lambda = \lambda_{emi}-\lambda_{exi}$).[55] A higher $\Delta\lambda$ value such as 60 nm is indicative of the characteristics of tryptophan residues while a lower $\Delta\lambda$ value such as 15 nm is characteristics of tyrosine residues.[56,57] We recorded the synchronous fluorescence spectra of bovine serum albumin with various concentrations of our compounds at $\Delta\lambda=15$ nm and $\Delta\lambda=60$ nm. It has been observed that there was a decrease in the fluorescence intensity of BSA at 304 and 346 nm. This is an indication for the fact that the ligands and complexes induce a fluorescence quenching of tyrosine and tryptophan. The synchronous fluorescence spectra $\Delta\lambda=60$ nm showed in Figure 13.
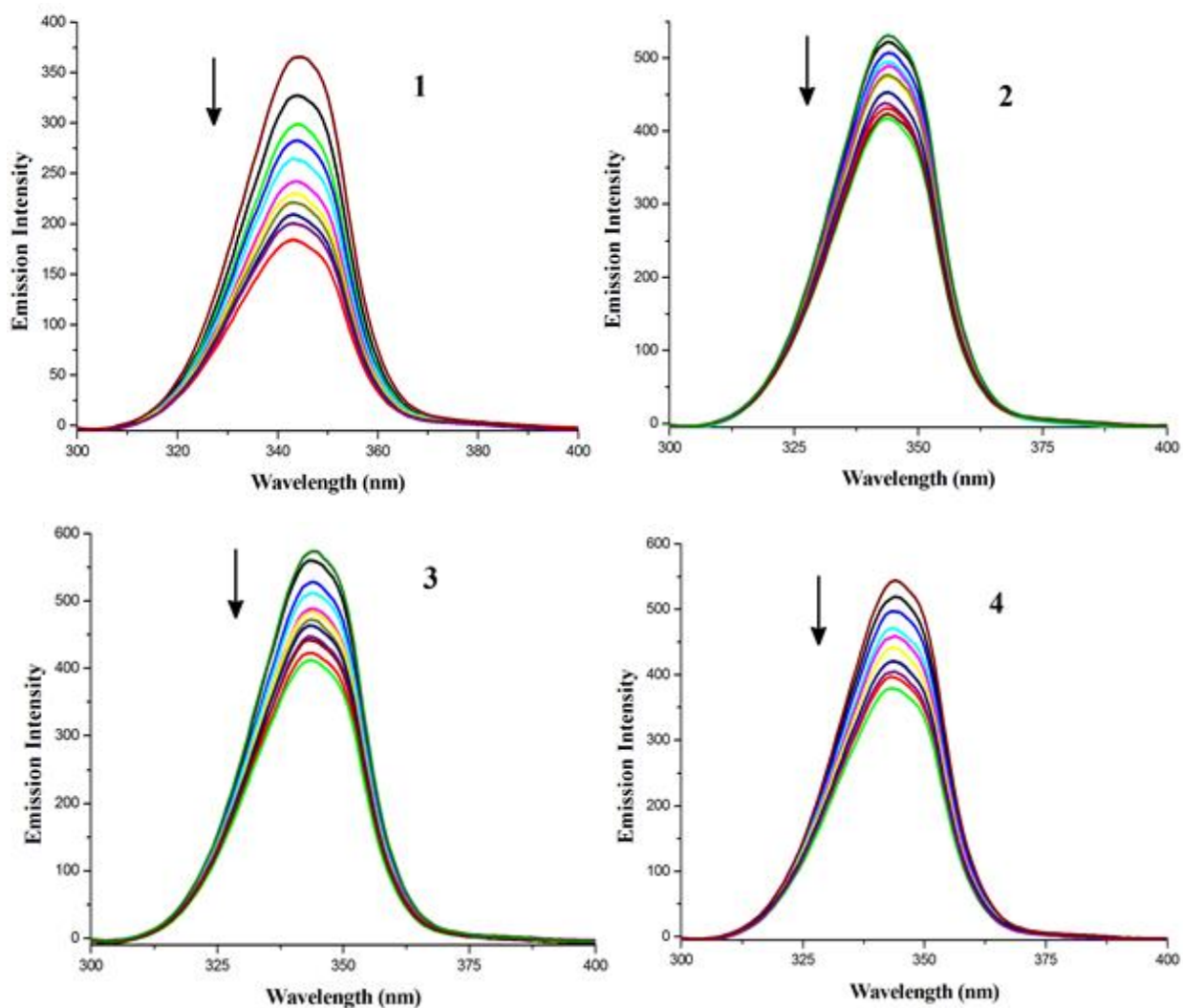

Figure 13. Synchronous fluorescence titration of BSA with the compounds at $\Delta\lambda=60$ nm.

Cytotoxicity

In order to find out the anticancer properties of the compounds, we carried out the cytotoxic investigations against the A549 (lung cancer) and MCF7 (breast cancer) cell lines in aqueous solution in comparison with the widely used drug doxorubicin and cisplatin under identical conditions by using an MTT assay. The results were analyzed by means of cell inhibition expressed as IC_{50} values and they are shown in Table 5 and Figure 14. After treated by the compounds, cancer cell lines change in morphology, and the observed morphological changes showed in Figure 15. From the results obtained, it has been noted that dicopper(II) complex **3** possessed the most potent inhibitory effect against the MCF7 cell line, when its IC_{50} value is compared with that of well-known anticancer drugs doxorubicin and cisplatin. The morphological changes examined by staining method suggested that the cell death mechanism was through apoptosis. Interestingly, the order of the *in vitro* anticancer activities of the two copper(II) complexes against selected cancer cell lines are in accordance with their DNA and protein binding abilities, suggesting that the anticancer activities of the two copper(II) complexes may have come from the strong hydrophobic interaction of the compounds with both DNA and protein binding. The order of cytotoxicity is doxorubicin > cisplatin> **3** > **4** > **2** > **1** for A549 cell line and doxorubicin > cisplatin > **3** > **4** > **1** > **2** for MCF7 cancer cell lines.[58-60]

Table 5. The IC_{50} values of the compounds

Compound	IC_{50} values (μM)	
	A-549	MCF-7
1	34 ± 0.8	33 ± 1.4
2	30 ± 0.9	35 ± 1.5
3	26 ± 1.5	23 ± 0.7
4	29 ± 1.1	26 ± 1.4
Doxorubicin	15 ± 1.2	16 ± 1.3
Cisplatin	25 ± 2.13	18.7 ± 0.1
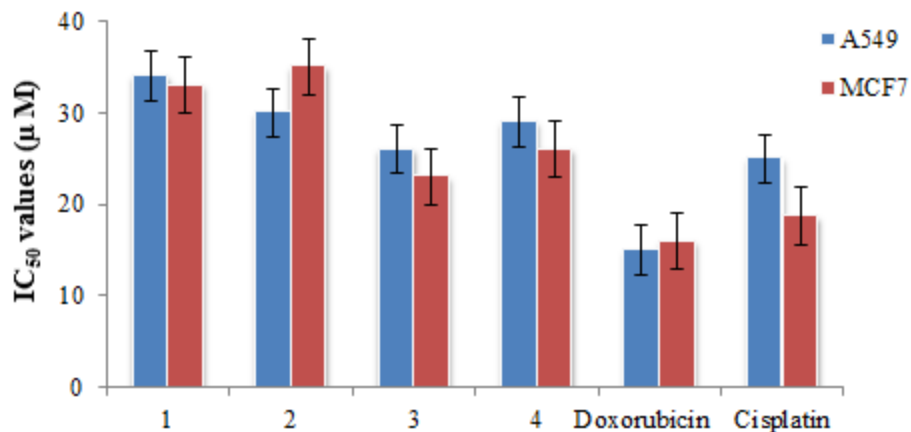
Figure 14. IC$_{50}$ values of compounds against A549 and MCF7cell lines.
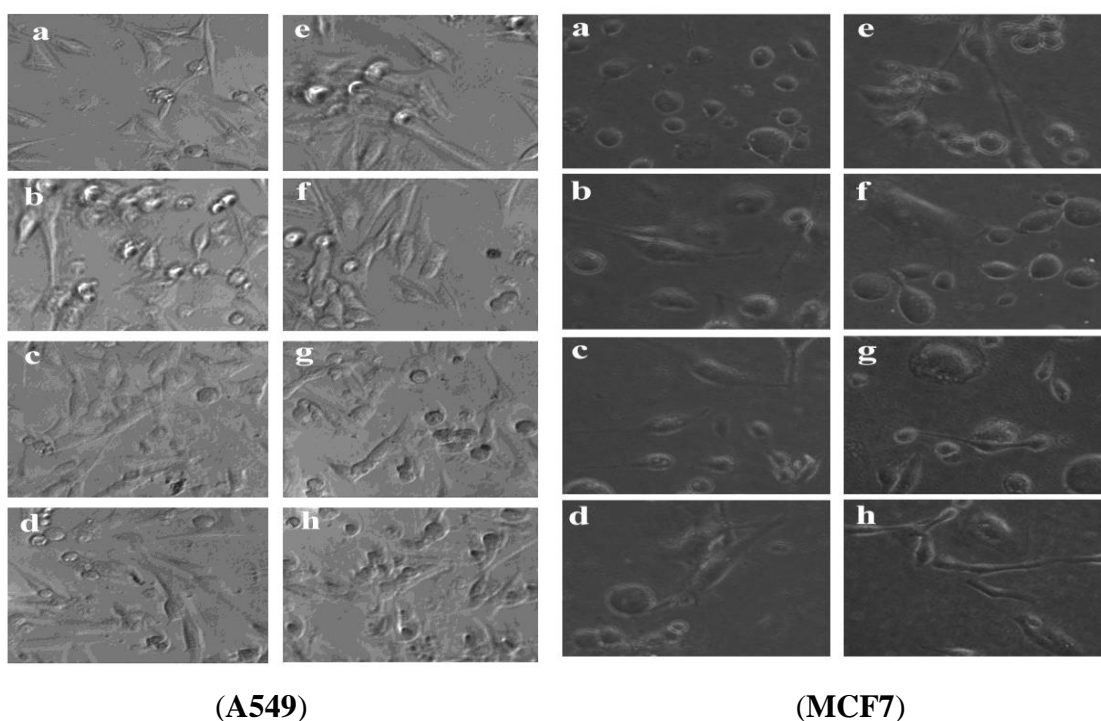

(A549)   **(MCF7)**

Figure 15. Morphological changes observed in the A549 and MCF7 (a, b, c, d control) cells at 24 h incubation by the treatment of compounds (**1-4**) (e, f, g, h treated cells).

Morphological changes in AO/EB and DAPI fluorescence study

In the designing of potential anticancer drugs, it is important to consider the apoptotic pathways. Apoptosis induction is an anti-proliferative mechanism by which the cancer cells undergo programmed death and is very beneficial if the new compounds trigger the death of cancer cells by apoptosis. To obtain a clear information, it is necessary to characterize the cells undergoing apoptosis by morphological and biochemical changes including cell shrinkage, chromatin

condensation and DNA fragmentation.[61] In this connection, the ability of apoptotic cells to increase the plasma membrane permeability to certain fluorescent dyes, e.g., AO/EB, Hoechst, AO/PI, DAPI etc., is made use of and we studied AO/EB and DAPI staining assays.[62] The morphological changes observed in the treated cells are classified into four types on the basis of the fluorescence emission and morphological features of chromatin condensation in the AO/EB stained nuclei. All these morphological changes were observed after treatment of the cancer cells with the ligands and complexes and the changes observed are shown in Figure 16. From the figure it can be seen that the green colour of the cells has been converted into orange/red colour cells showing an early apoptotic cells with membrane blebbing, which is seen at fixed concentration of compounds and untreated A549 and MCF7 cancer cells (control) did not show any significant adverse effect as compared to the ones treated by compounds. From DAPI fluorescence staining studies, the blue bright patches formed indicates the condensed chromatins and nuclear fragmentations in the cancer cells. Further, it is to be also noted that the bright blue patches observed in compounds are higher when compared that with untreated A549 and MCF7 cells showed in Figure 17. The observed results do indicate that complexes **3** and **4** induced cell death by apoptosis which is in good agreement with the above cytotoxicity results.
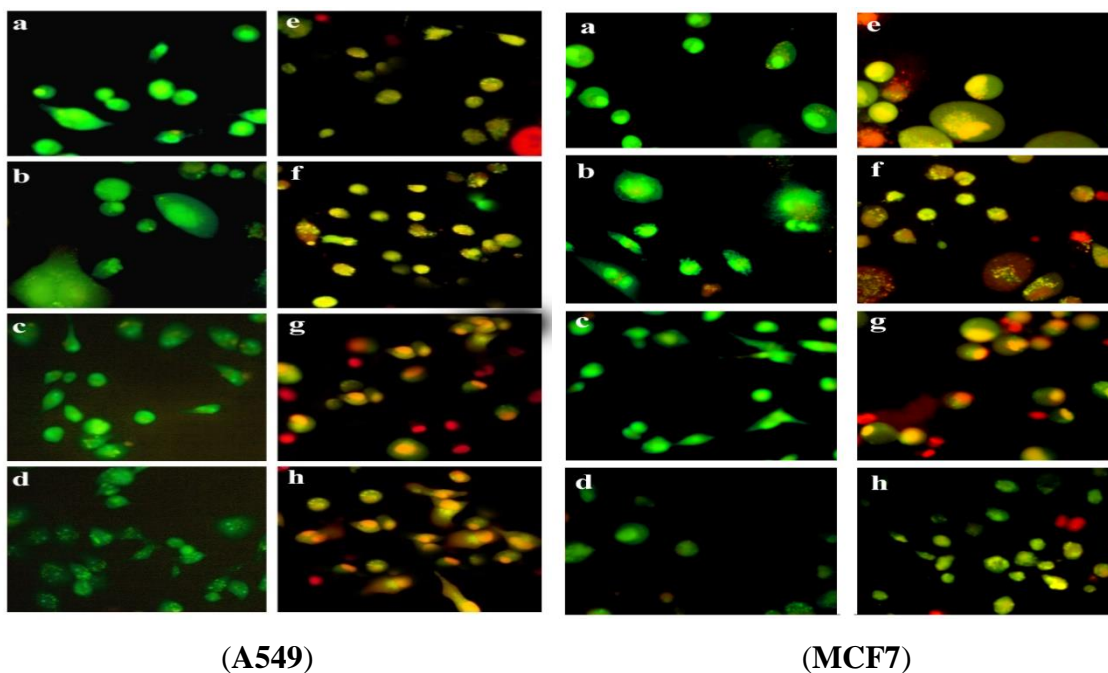

(**A549**)   (**MCF7**)

Figure 16. AO/EB stained A549 and MCF7 (a, b, c, d control) cells at 24 h incubation by the treatment of compounds (**1-4**) (e, f, g, h treated cells). The yellow and red patches indicate early apoptotic in the cancer cells.
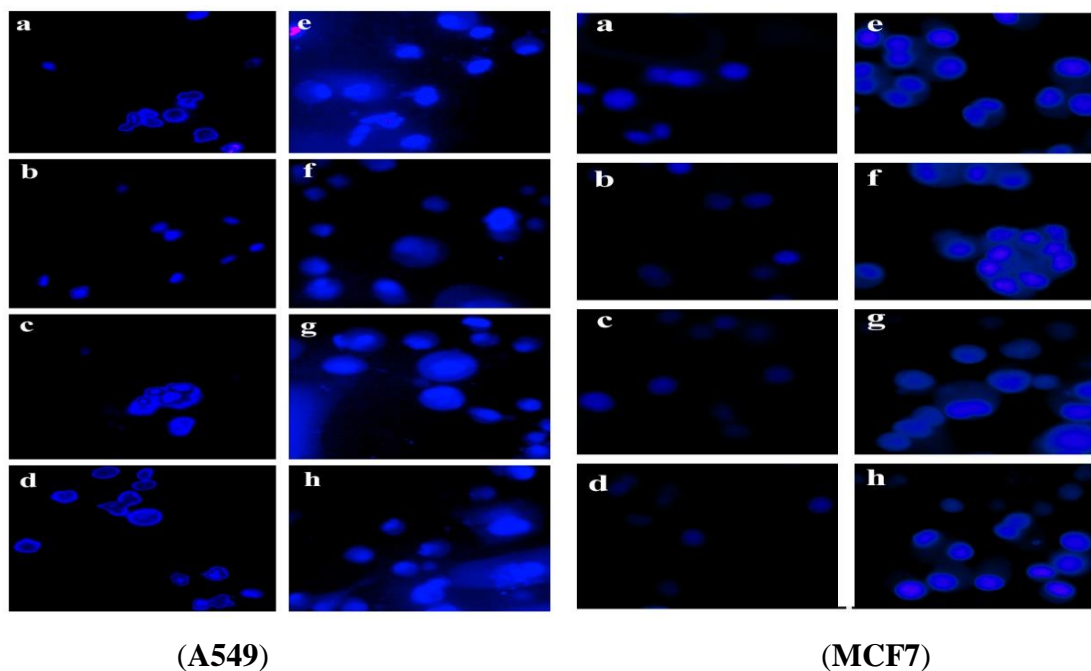

(**A549**)   (**MCF7**)

Figure 17. DAPI stained A549 and MCF7 (a, b, c, d control) cells at 24 h incubation by the treatment of compounds (**1-4**) (e, f, g, h treated cells). The bright blue patches show condensed chromatins and nuclear fragmentations in the cancer cells.

Conclusion

In summary, this work highlights the synthesis, characterization and detailed biological studies of a water soluble chloro bridged binuclear copper(II) complex (**3**) and mononuclear complex (**4**) prepared from the reaction of chloro substituted 2-oxo-1,2-dihydroquinolin-3-yl-methylene-2 hydroxybenzohydrazide and $CuCl_2 \cdot 2H_2O$. The ligand coordinates to copper ion in a tridentate (ONO) manner. The single crystal structures of the complex **3** and **4** indicated square pyramidal geometry for both the complexes. The binding abilities of the new complexes with CT-DNA and BSA have been investigated by using absorption and fluorescence spectroscopic methods. The results indicated that the compounds bind to CT-DNA *via* intercalation mode and the intrinsic fluorescence of BSA was quenched by a static quenching mechanism *via* hydrophobic interaction. All the compounds showed significant *in vitro* cytotoxic activity against A549 (lung cancer) and MCF7 (breast cancer) cell lines. The morphological changes examined by staining

method suggested that the mechanism of cell death was through apoptosis. From the results of the above biological studies, we observed that complex **3** has the most significant activity, which may be due to the greater planar area that the complex **3** has when compared to that of the others. The findings do indicate that the complex **3** may have potential practical applications for pharmaceutical development in the future.

Acknowledgement

References

[1] P. K. Radhakrishnan, P. Indrasenan, C. G. R. Nair, *Polyhedron* **1984**, 3, 67

[2] C. Liu, M. Wang, T. Zhang, H. Sun, *Coord. Chem. Rev*. **2004**, 248, 147.

[3] B. Lippert, *Coord. Chem. Rev*. **2000**, 200, 487.

[4] X. B. Yang, J. Feng, J. Zhang, Z. W. Zhang, H. H. Lin, L. H. Zhou, X. Q. Yu, *Bioorgan. Med. Chem.* **2008**, 16, 3871.

[5] S. Gama, F. Mendes, F. Marques, *J. Inorg. Biochem*. **2011**, 105, 637.

[6] S. Banerjee, S. Mondal, S. Sen, *Dalton Trans*. **2009**, 46, 6849.

[7] N. J. Garrido, L. Perello, R. Ortiz, *J. Inorg. Biochem*. **2005**, 99, 677.

[8] D. Lahiri, S. Roy, S. Saha, *Dalton Trans*. **2010**, 39, 1807.

[9] D. Charles, J. H. Turner, C. Redmond, *BJOG – Int. J. Obstet. Gy*. **2005**,80, 264.

[10] P. J. Sorbie, R. Perez-Marrero, Review article, *J. Urol*. **1984**, 131, 425.

[11] E. L. Hegg, J. N. Burstyn, *Coord. Chem. Rev*. **1998**, *173*, 133.

[12] F. Mancin, P. Scrimin, P. Tecilla, U. Tonellato, *Chem. Commun*. **2005**, 2540.

[13] D. S. Sigman, T. W. Bruce, C. L. Sutton, *Acc. Chem. Res*. **1993**, *26*, 98.

[14] W. K. Pogozelski, T. D. Tullius, *Chem. Rev*. **1998**, *98*, 1089.

[15] B. Armitage, *Chem. Rev*. **1998**, *98*, 1171.

[16] S. Dhar, D. Senapati, P. K. Das, P. Chattopaddhyay, M. Nethaji, A. R. Chakravarty, *J. Am. Chem. Soc*. **2003**, *125*, 12118.

[17] P. M. Bradley, A. M. Angeles-Boza, P. K. L. Fu, K. R. Dunbar, C. Turro, *Inorg. Chem*. **2004**, *43*, 2450.

[18] P. U. Maheswari, S. Roy, H. D. Dulk, S. Barends, G. V. Wezel, B. Kozlevcar, P. Gamez, J. Reedijk, *J. Am. Chem. Soc*. **2006**, *128*, 710.

[19] Q. Jiang, N. Xiao, P. F. Shi, Y. G. Zhu, Z. J. Guo, *Coord. Chem. Rev*. **2007**, *251*, 1951.

[20] X. F. Zhao, Y. Ouyang, Y. Z. Liu, Q. J. Su, H. Tian, C. Z. Xie, J. Y. Xu, *New J. Chem*. **2014**, *38*, 955.

[21] X. D. Dong, X. Y. Wang, M. X. Lin, H. Sun, X. L. Yang, Z. J. Guo, *Inorg. Chem.* **2010**, *49*, 2541.

[22] P. Kumar, S. Gurai, M. K. Santra, B. Mondal, D. Manna, *Dalton Trans*. **2012**, *41*, 7573.

[23] Y. Hu, Y. Yang, C. Dai, Y. Liu, X. Xiao, *Biomacromolecules*, **2010,** *11*, 106.

[24] C. Santini, M. Pellei, V. Gandini, M. Porchia, F. Tisato, C. Marzano, *Chem. Rev*. **2014**, *114*, 815.

[25] (a) M. Sutradhar, G. Mukherjee, M. G. B. Drew, S. Ghosh, *Inorg. Chem*. **2007**, *46*, 5069. (b) M. Sutradhar, L. M. Carrella, E. Rentschler, *Eur. J. Inorg. Chem*. **2012**, *4*, 4273. (c) T. Roy Barman, M. Sutradhar, M. G. B. Drew, E. Rentschler, *Polyhedron*, **2013**, *51*, 192. (d) M. Sutradhar, T. Roy Barman, J. Klanke, M. G. B. Drew, E. Rentschler, *Polyhedron*, **2013**, *53*, 48.

[26] (a) R. K. Hocking, E. I. Solomon, Molecular Electronic Structures of Transition Metal Complexes, ed. D. M. P. Mingos, P. Day, J. P. Dahl, *Springer,* NY, USA, **2012**, *142*, 155. (b) R. H. Crabtree, The *Organometallic Chemistry of the Transition Metals, John Wiley & Sons,* **2011**. (c) M. Shatruk, C. Avendano, K. R. Dunbar, *Inorg. Chem. ed*. K. D. Karlin, John Wiley & Sons, NY, USA, **2009**, *56*, 155. (d) R. Boca, A Handbook of Magneto Chemical Formulae, *Elsevier,* Amsterdam, 2012, J. Jezierska, O. V. Nesterova, A. J. L. Pombeiro, A. Ozarowski, *Chem. Commun.,* **2014**, *50*, 3431. (f) J. R. J. Sorenson, Biology of Copper Complexes, Humana Press, **2011**.

[27] J. Tan, B. Wang, L. Zhu, *Bioorg. Med. Chem*. **2009**, *17*, 614.

[28] B. P. Esposito, R. Najjar, *Coord. Chem. Rev*. **2002**, *232*, 137.

[29] N. Bharti, M. R. Maurya, F. Naqvi, A. Bhattacharya, S. Bhattacharya, A. Azam, *Eur. J. Med. Chem.* **2000**, *35*, 481.

[30] (a) E. Kimoto, H. Tanaka, J. Gyotoku, F. Morishige, L. Pauling, *Cancer Res*. **1983**, *43*, 824. (b) R. I. Maurer, P. J. Blower, J. R. Dilworth, C. A. Reynolds, Y. Zheng, G. E. D. Mullen, *J. Med. Chem.* **2002**, *45*, 1420. (C) P. A. N. Reddy, M. Nethaji, A. R. Chakravarty, *Eur. J. Inorg. Chem.* **2004**, *7*, 1440.

[31] C. N. Hancock, L. H. Stockwin, B. Han, R. D. Divelbiss, J. H. Jun, S. V. Malhotra, M. G. Hollingshead, D. L. Newton, *Free Radical Biol. Med*. **2011**, *50*, 110.

[32] M. K. Singh, A. Chandra, B. Singh, R. M. Singh, *Tetrahedron Lett.* **2007**, *48*, 5987.

[33] A. I. Vogel, Text Book of Practical Organic Chemistry, 5th Ed. Longman. London, **1989**.

[34] R. Prabhakaran, P. Kalaivani, P. Poornima, F. Dallemer, G. Paramaguru, V. Vijaya Padma, R. Renganathan, R. Huang, K. Natarajan, *Dalton Trans*. **2012**, *41*, 9323.

[35] P. Kalaivani, C. Umadevi, R. Prabhakaran, F. Dallemer, P. S. Mohan, *Inorganica Chimica Acta*, **2015**, *438*, 264.

[36] (a) M. Blagosklonny, W. S. EIdiery, *Int. J. Cancer*, **1996**, *67*, 386. (b) P. Vijayan, P Viswanathamurthi, P. Sugumar, M. N. Ponnuswamy, M. D. Balakumaran, P. T. Kalaichelvan, K. Velmurugan, R. Nandhakumard, R. J. Butchere, *Inorg. Chem. Front*. **2015**, *2*, 620.

[37] O.V. Dolomanov, L. J. Bourhis, R. J. Gildea, J. A. K. Howard, H. Puschmann, Olex2: A complete structure solution, refinement and analysis program, *J. Appl. Cryst.* **2009**, *42*, 339.

[38] Sheldrick, G.M., A short history of ShelX, *Acta Cryst.* **2008**, *A64*, 339.

[39] CrysAlisPro Software System, Agilent Technologies UK Ltd, Yarnton, Oxford, UK, **2014**.

[40] (a) M. Hazra, T. Dolai, A. Pandey, S. K. Dey, A. Patra, *Bioinorg. Chem. Appl*, **2014**, 104046. (b) K. Alomar, M. A. Khan, M. Allain and G. Bouet, *polyhedron*, **2009**, *28*, 1273. (c) Y.P. Tiam, C.Y. Duan, Z.L. Lu and X.Z. You, *Polyhedron*, **1996**, *15*, 2263.

[41] N. Sengottuvelan, D. Saravanakumar, M. Kandaswamy, *Polyhedron* **2007**, *26*, 3825.

[42] D. Senthil Raja, N. S. P. Bhuvanesh, K. Natarajan, *Eur. J. Inorg. Chem*, **2012**, *47*, 73.

[43] D. Senthil Raja, N. S. P. Bhuvanesh, K. Natarajan, *Eur. J. Inorg.* Chem, **2013**, *64*, 148

[44] A. F. Tanious, D. Y. Ding, D. A. Patrick, C. Bailly, R. R. Tidwell, W. D. Wilson, *Biochemistry* **2000**, *39*, 12091.

[45] C. Y. Zhong, J. Zhao, Y. B. Wu, C. X. Yin, P. J. Yang, *Inorg. Biochem.* **2007**, *101*, 1347.

[46] A. Wolfe, G. H. Shimer, T. Meehan, *Biochemistry* **1987**, *26*, 6392.

[47] J. S. Guerrero, P. C. Sanchez, E. R. Perez, F. V. Garcia, M. E. B. Gomez, L. R Azuara, *Toxicol in vitro* **2011**, *25*, 1376.

[48] P. J. Cox, G. Psomas, C. A. Bolos, *Bioorg. Med. Chem.* **2009**, *17*, 6054.

[49] (a) M. J. Waring, *J. Mol. Biol*, **1965**, *13*, 269. (b) I. Changzheng, W. Jigui, W. Liufang, R. Min, J. Naiyang, G. Jie, *J. Inorg. Biochem.* **1999**, *73*, 195. (c) M. Lee, A. L. Rhodes, M. D. Wyatt, S. Forrow, J. A. Hartley, *Biochemistry* **1993**, *32*, 4237.

[50] K. A. Z. Osama, I. K. A. S. Othman, *J. Am. Chem. Soc*. **2008**, *130*, 10793.

[51] D. S. Raja, G. Paramaguru, N. S. P. Bhuvanesh, J. H Reibenspies, R. Renganathan, K. Natarajan, *Dalton Trans.* **2011**, *40*, 4548.

[52] D. S. Raja, N. S. P. Bhuvanesh, K. Natarajan, *Eur. J. Med. Chem.* **2011**, *46*, 4584.

[53] (a) P. J. Cox, G. Psomas, C. A. Bolos, *Bioorg. Med. Chem*. **2009**, *17*, 6054. (b) M. J. Waring, *J. Mol. Biol*. **1965**, *13*, 269. (c) I. Changzheng, W. Jigui, W. Liufang, R. Min, J. Naiyang G. Jie, *J. Inorg. Biochem*. **1999**, *73*, 195.

[54] P. Krishnamoorthy, P. Sathyadevi, A. H. Cowley, R. R. Butorac, N. Dharmaraj, *Eur. J. Med. Chem*. **2011**, *46*, 3376.

[55] J. N. Miller, *Proc. Anal. Div. Chem. Soc*. 1979, 16, 203.

[56] F. J. Meyer-Almes, D. Porschke, *Biochemistry* **1993**, *32*, 4246.

[57] Z. C. Liu, B. D. Wang, B. Li, Q. Wang, Z. Y. Yang, T. R. Li, Y. Li, *Eur. J. Med. Chem*. **2010**, *45*, 5353.

[58] D. S. Raja, N. S. P. Bhuvanesh, K. Natarajan, *Inorg. Chem*. **2011**, *50*, 12852.

[59] S. Roy, P. U. Maheswari, M. Lutz, A. L. Spek, H. den Dulk, S. Barends, G. P. van Wezel, F. Hartl, J. Reedijk, *Dalton Trans*. **2009**, 10846

[60] S. Gama, F. Mendes, F. Marques, I. C. Santos, M. F. Carvalho, I. Correia, J. C. Pessoa, I. Santos, A. Paulo, *J. Inorg. Biochem*. **2011**, *105*, 637.

[61] D. Baskic, S. Popovic, P. Ristic, N. N. Arsenijevic, *Cell Biol. Int. Rep*. **2006**, *30*, 924.

[62] H. L. Chan, D. L. Ma, M. Yang, C. M. Che, *ChemBio- Chem*. **2003**, *4*, 62.